

Argonaute proteins regulate HIV-1 multiply spliced RNA and viral production in a Dicer independent manner

Agathe Eckenfelder, Emmanuel Ségéral, Natalia Pinzón, Damien Ulveling, Céline Amadori, Marine Charpentier, Sabine Nidelet, Jean-Paul Concordet, Jean-François Zagury, Jc Paillart, et al.

▶ **To cite this version:**

Agathe Eckenfelder, Emmanuel Ségéral, Natalia Pinzón, Damien Ulveling, Céline Amadori, et al.. Argonaute proteins regulate HIV-1 multiply spliced RNA and viral production in a Dicer independent manner. Nucleic Acids Research, 2017, 45 (7), pp.4158-4173. 10.1093/nar/gkw1289 . hal-01539171

HAL Id: hal-01539171
https://hal.science/hal-01539171

Submitted on 14 Jun 2022

HAL is a multi-disciplinary open access archive for the deposit and dissemination of scientific research documents, whether they are published or not. The documents may come from teaching and research institutions in France or abroad, or from public or private research centers.

L'archive ouverte pluridisciplinaire **HAL**, est destinée au dépôt et à la diffusion de documents scientifiques de niveau recherche, publiés ou non, émanant des établissements d'enseignement et de recherche français ou étrangers, des laboratoires publics ou privés.



Distributed under a Creative Commons Attribution 4.0 International License

4158–4173 *Nucleic Acids Research, 2017, Vol. 45, No. 7* *Published online 21 December 2016*
doi: 10.1093/nar/gkw1289

Argonaute proteins regulate HIV-1 multiply spliced RNA and viral production in a Dicer independent manner

Agathe Eckenfelder[1,2,3], Emmanuel Ségéral[1,2,3], Natalia Pinzón[4], Damien Ulveling[5], Céline Amadori[1,2,3], Marine Charpentier[6], Sabine Nidelet[7], Jean-Paul Concordet[6], Jean-François Zagury[5], Jean-Christophe Paillart[8], Clarisse Berlioz-Torrent[1,2,3], Hervé Seitz[4], Stéphane Emiliani[1,2,3,*] and Sarah Gallois-Montbrun[1,2,3,*]

[1]INSERM, U1016, Institut Cochin, Paris 75014, France, [2]CNRS, UMR8104, Paris 75014, France, [3]Université Paris Descartes, Sorbonne Paris Cité, Paris 75006, France, [4]CNRS, UPR 1142, Institut de Génétique Humaine, Montpellier 34396, France, [5]CNAM, Laboratoire Génomique, Bioinformatique et Applications (EA 4627), Paris 75003, France, [6]INSERM, U1154, CNRS, UMR7196, Museum National d'Histoire Naturelle, Paris 75231, France, [7]Plateforme MGX, Institut de Génomique Fonctionnelle, CNRS, UMR5203, INSERM, U661, Montpellier 34094, France and [8]Architecture et Réactivité de l'ARN, Université de Strasbourg, CNRS, IBMC, Strasbourg 67084, France

Received January 14, 2016; Revised November 21, 2016; Editorial Decision December 08, 2016; Accepted December 13, 2016

ABSTRACT

Argonaute (Ago) proteins associate with microRNAs (miRNAs) to form the core of the RNA-induced silencing complex (RISC) that mediates post-transcriptional gene silencing of target mRNAs. As key players in anti-viral defense, Ago proteins are thought to have the ability to interact with human immunodeficiency virus type 1 (HIV-1) RNA. However, the role of this interaction in regulating HIV-1 replication has been debated. Here, we used high throughput sequencing of RNA isolated by cross-linking immunoprecipitation (HITS-CLIP) to explore the interaction between Ago2 and HIV-1 RNA in infected cells. By only considering reads of 50 nucleotides length in our analysis, we identified more than 30 distinct binding sites for Ago2 along the viral RNA genome. Using reporter assays, we found four binding sites, located near splice donor sites, capable of repressing Luciferase gene expression in an Ago-dependent manner. Furthermore, inhibition of Ago1 and Ago2 levels in cells expressing HIV-1 led to an increase of viral multiply spliced transcripts and to a strong reduction in the extracellular CAp24 level. Depletion of Dicer did not affect these activities. Our results highlight a new role of Ago proteins in the control of multiply spliced HIV-1 transcript levels and viral production, independently of the miRNA pathway.

INTRODUCTION

More than 100 different viral transcripts have been identified in HIV-1 infected cells by deep sequencing (1). These transcripts are generated through alternative splicing of a single primary transcript of approximately 9-kb in size. This unspliced (US) pre-mRNA can either be packaged into viral particles as viral genomic RNA (gRNA) or used as mRNA for the production of Gag and Gag/Pol proteins. It can also be processed through the presence of four major splice donor sites (SD1–SD4) and seven acceptor sites (SA1–SA7). Additional cryptic donor and acceptor sites have also been identified. Spliced RNAs can be divided in two classes: multiply spliced (MS) RNAs (of ∼1.8-kb) that are produced early during infection and that encode the regulatory viral proteins Tat, Rev and Nef and singly spliced (SS) mRNAs (of ∼4-kb) that are produced as the infection progresses for the synthesis of Env, as well as auxiliary proteins Vif, Vpr and Vpu. HIV-1 splicing has to be highly orchestrated to allow the balanced production of viral RNAs and proteins. Splicing efficiency is dependent on the sequence of the 5′ splice site and its degree of complementarity to U1 snRNA. In addition, the presence of splicing regulator elements nearby splicing acceptor sites allows the recruitment of cellular factors that interact with the splicing machinery. These factors belong for the majority to the splicing regulatory hnRNP or serine/arginine (SR)-rich protein families that either promote or repress splicing. Splicing is also influenced by local structures of the splicing donor sites (2,3).

*To whom correspondence should be addressed. Tel: +33 140516576; Fax: +33 140516570; Email: sarah.gallois-montbrun@inserm.fr
Correspondence may also be addressed to Stéphane Emiliani. Tel: +33 140516639; Fax: +33 140516570; Email: stephane.emiliani@inserm.fr

© The Author(s) 2016. Published by Oxford University Press on behalf of Nucleic Acids Research.
This is an Open Access article distributed under the terms of the Creative Commons Attribution License (http://creativecommons.org/licenses/by-nc/4.0/), which permits non-commercial re-use, distribution, and reproduction in any medium, provided the original work is properly cited. For commercial re-use, please contact journals.permissions@oup.com

Downloaded from https://academic.oup.com/nar/article/45/7/4158/2726865 by BIU Montpellier user on 14 June 2022

Argonautes are highly conserved proteins that play a key role in gene-silencing pathways via direct interaction with small non-coding RNAs such as short interfering RNAs, microRNAs (miRNAs) and PIWI-interacting RNAs. In humans, eight Argonaute proteins are divided in two families, the Argonaute (Ago) subfamily that comprises Ago1 through Ago4 and the PIWI subfamily. MiRNAs are 19 to 24 nucleotides single stranded RNAs typically generated from precursor miRNAs by the RNAseIII enzyme Dicer. MiRNAs associate with one of the four Ago proteins leading to the formation of the RNA induced silencing complex (RISC). Once loaded into the RISC, the miRNA targets specific regions of mRNAs. The binding of Ago proteins to the transcripts in the cytoplasm results in post-transcriptional gene silencing (4). In addition to their role in post-transcriptional gene silencing, several studies have recently reported that Ago1 and Ago2 can also exert nuclear functions in mammalian cells such as RNA-mediated transcriptional gene silencing (5–8), transcriptional gene activation (9,10), DNA repair (11,12) and regulation of alternative splicing. Kornblihtt *et al*. originally reported that duplex RNAs targeting pre-mRNA could regulate alternative exon inclusion. This effect required Ago1 and correlated with an increase in local heterochromatin marks (13). Subsequent work in Drosophila and human cells showed that Ago1 and Ago2 proteins have the ability to control alternative splicing patterns of many cellular transcripts (14–16).

Several evidences also support a role of the small RNA pathways interplay in HIV-1 replication (17). However, its real implication is still debated. Studies indicated that HIV infection alters the expression of cellular miRNAs (18–21), even if these effects appear limited at early times after infection (22). Furthermore, specific cellular miRNAs were identified to target the HIV genome and to inhibit viral replication (23–25) and effector proteins of the RNAi pathway were shown to be involved in the inhibition of HIV-1 viral production and/or infectivity (25–27). However, a report from Bogerd *et al*. suggested a moderate role, if any, of miRNA in HIV viral particle production and infectivity (28). HIV-1-derived small non-coding RNAs (sncRNAs) were identified in HIV-1 infected cells by deep sequencing, but their level of expression was relatively low compared to total small RNAs (22,29–32). In addition, the size of these viral sncRNAs is somehow heterogeneous and does not cluster at the 22 ± 2 nt size usually observed for cellular miRNAs suggesting that these viral products are not directly involved in small RNA canonical pathways (22). HIV-1 transcripts were shown to associate with Ago2 using RNA immunoprecipitation approaches (25,26,33). Furthermore, although high-throughput sequencing of RNAs isolated by cross-linking immunoprecipitation failed to detect the presence of viral sncRNA associated with Ago2-RISC in infected macrophages (32), Ago binding sites on HIV-1 RNA genome were identified in HeLa and CD4+ lymphocyte cells infected with HIV-1 (22). Knockdown of Ago2 expression decreases the production of virions (33,34) and partial simultaneous knockdown of the 4 Ago proteins in HIV-1 producer cells also resulted in moderate decrease in viral production, and a 4-fold increase of the infectivity of progeny virions (27). However, the mechanisms by which Ago affects the viral replication and the importance of miRNA in this process remain unclear.

In this study, we aimed to clarify the role of Ago2 in HIV-1 infection. We showed that Ago2 binds preferentially to unspliced HIV-1 pre-mRNA. By using an Ago2-HITS-CLIP strategy, we identified distinct regions of HIV-1 RNA that are associated to Ago2-RISC. In particular, several Ago2 binding regions overlapping with the HIV-1 splice donor sites in the context of the viral gRNA were functionally validated using a dual reporter assay. The recruitment of Ago proteins on these regions appears to be independent on the presence of miRNAs. We characterized the effect of Ago1 and Ago2 downregulation on HIV-1 mRNA levels and showed that Ago proteins modulate the production of multiply spliced viral transcripts. Ago proteins are also involved in the production of viral particles. Both effects appeared to be independent on the miRNA pathway.

MATERIALS AND METHODS

Cell culture

HEK293T, HeLa, HeLa P4.2 and HeLa TZM-bl cells were cultivated at 37°C and 5% CO_2 in Dulbecco's modified Eagle's medium medium (Life Technologies) supplemented with 10% fetal calf serum (Life Technologies). Jurkat cells were cultivated at 37°C and 5% CO_2 in RPMI medium (Life Technologies) supplemented with 10% fetal calf serum (Life Technologies).

Knockout and knockdown cell lines

pTAL-DicerL and pTAL-DicerR plasmids were assembled into the pTALEN-V2 backbone according to the Unit Assembly Methodology (modified from (35)). These constructs allow the expression of a TALEN nuclease pair targeting the following sequence of the second exon of human *Dicer1* gene: t**tctgctgaagtctccc**ctgatctgataggacag**ctctttagtgagtagt**a (with TALEN-DicerL and TALEN-DicerR binding site sequences indicated in bold). HeLa P4.2 cells were transfected with pTAL-DicerR and pTAL-DicerL using Lipofectamine LTX (Life technologies) and incubated for 24 h. To increase TALEN efficiency, they were transferred at 30°C for 3 days. The next day, single cells were isolated using a BD Biosciences FACSAria III. Clonal populations were expanded, and whole cell extracts were screened for Dicer depletion by sodium dodecyl sulphate-polyacrylamide gel electrophoresis (SDS-PAGE) and immunoblotting using anti-Dicer antibody (N167/7, Merck Millipore). One Dicer knockout cellular clone (Dicer KO) was selected for further analysis.

LentiCRISPRv2-Ago2 expression plasmid expressing single-guide RNA targeting exon 2 of *Ago2* gene was generated by annealing and cloning the following primers: caccgtcaagccagagaagtgcccg and aaaccgggcacttctctggcttgac into the lentiCRISPRv2 (36). HEK293T cells were transfected either with lentiCRISPRv2-Ago2 or empty lentiCRISPRv2 as control using Lipofectamine LTX (Life technologies). Forty-eight hours later, viral particles were harvested and used to transduce HeLa cells. Cells were selected in medium supplemented with puromycin for 15 days. Cells

Downloaded from https://academic.oup.com/nar/article/45/7/4158/2726865 by BIU Montpellier user on 14 June 2022

transduced with empty lentiCRISPRv2 were used as control cells. Data acquisition and data analysis were performed on the Cochin Cytometry and Immunobiology core Facilities. Single cells were isolated from lentiCRISPRv2-Ago2 transduced cells using a BD Biosciences FACSAria III and expression of Ago2 in the cell clones was analyzed by SDS-PAGE and immunoblotting. One cell clone knockout for Ago2 (Ago2 KO) was selected for further analysis.

Ago2 KO cells were transduced with shRNA against Ago1 and selected with puromycin for 7 days. As control, HeLa cells transduced with empty lentiCRISPRv2 were transduced with shRNA scramble. Inhibition of Ago1 and Ago2 expression was monitored by Western blot analysis using anti-Ago1 (4B8, Merck Millipore), anti-Ago2 (11A9, Merck Millipore) and anti-Tubulin (Sigma Aldrich) antibodies.

Virus stock production

Stocks of VSVg pseudotyped NL4-3 HIV-1 viruses were generated by transfecting 3×10^6 HEK293T cells with pNL4-3 and VSVg (pMD.G) expression vectors using polyethylenimine (PEI) (PolySciences). Virus-containing supernatant was collected 48 h later, filtered and purified by ultracentrifugation on a sucrose cushion. HIV-1 CAp24 was quantified by ELISA (Perkin Elmer). Infectious viral titers were assessed by infection of HEK293T or Jurkat cells with a serial dilution of virus stocks. Twenty-four hours post-infection, intracellular CAp24 was immunostained with an anti-CAp24 antibody (KC57-FITC, Coulter) and the percentage of infected cells determined by FACS analysis.

Cross-linking and immunopurification (CLIP) of endogenous Ago2

A total of 15×10^6 Jurkat cells were infected with VSVg pseudotyped HIV-1 viruses at a multiplicity of infection (M.O.I.) of 1. Twenty-four hours later, infected cells were rinsed, resuspended in ice cold 1X phosphate buffered saline (PBS) and irradiated at 400 mJ/cm^2 and 200 mJ/cm^2 subsequently using a Stratalinker 2400. Cell pellets were frozen at −80°C, thawed on ice in lysis buffer (1X PBS, 0.5% NP40, 6 mM $MgCl_2$, 2 mM dithiothreitol, 1X complete ethylenediaminetetraacetic acid (EDTA)-free protease inhibitor (Roche)), digested with 60 U of Turbo DNaseI (Ambion) during 10 min at 37°C and centrifuged 10 min at 1000 rpm at 4°C. Aliquot of supernatant was kept for subsequent protein and RNA analysis before IP (input). The rest was incubated overnight with Protein G Dynabeads previously incubated with an anti-Ago2 antibody (11-A9, Merck Millipore) or a mixture of Rat IgGs as control. Dynabeads were washed 5 times with Wash buffer (5X PBS, 1% NP40, 1% Sodium Deoxycholate, 6 mM $MgCl_2$, 2 mM dithiothreitol, 0.1% SDS, 1X Complete EDTA-free protease inhibitor (Roche)) and resuspended in 1X PBS. One-fifth was kept for Western blot analysis and the rest was subjected to proteinase K digestion in PK/urea buffer (100 mM Tris-HCl pH 7.5, 50 mM NaCl, 10 mM EDTA and 7 M urea) containing 4 mg of proteinase K (Roche). Input fraction was digested similarly for RNA extraction. RNAs from CLIP and Input were extracted using TRIzol LS reagent (Life Technologies), and precipitated with ethanol:isopropanol (1:1 ratio) and GlycoBlue (Ambion). RNAs were quantified by RTqPCR.

Relative quantification of RNA by RTqPCR

RNAs were reverse transcribed using the High-Capacity cDNA Reverse Transcription Kit (Applied Biosystems) and quantified by real-time PCR with a LightCycler 480 SYBR Green I Master (Roche) using specific primers for genomic US, singly spliced (SS), multiply spliced (MS) and Total viral cDNA, as well as for IRF3, GAPDH and Actine cDNA (Supplementary Table S3) (37).

GFP-Ago2 HITS-CLIP

HITS-CLIP procedure was adapted from (38). Briefly, HEK293T cells were transfected with pT7-EGFP-C1-HsAgo2 or pT7-EGFP-C1 (a kind gift of Elisa Izaurralde's laboratory) using FuGENE 6 (Promega). Twenty-four hours post-transfection, cells were infected with VSVg pseudotyped HIV-1 viruses at M.O.I. of 1 or mock infected. Twenty-four hours later, a sample was collected to assess GFP or GFP-Ago2 expression and the level of infection by intracellular CAp24 staining. Flow cytometry confirmed that at least 75% of the cells productively expressing the protein of interest were infected. Cells were irradiated, pelleted, resuspended in lysis buffer supplemented with RNAsin (Ambion) and treated with Turbo DNaseI as described before. One-fifteenth of each sample was conserved as input for subsequent RNA extraction and cDNA library preparation. The rest was partially digested with 50 U of RNaseI (Ambion) for 7 min at 37°C. As a preclearing step, cell lysates were first incubated with uncoupled Dynabeads for 1 h 30 at 4°C. Precleared cell lysates were then incubated with Dynabeads previously coupled to an anti-GFP antibody (Roche). Dynabeads were washed 4 times with Wash buffer supplemented with 4 M urea and twice with 1 ml of PNK buffer (10 mM $MgCl_2$, 0.2% Tween20, 20 mM Tris-HCl pH7.4). RNAs were dephosphorylated on beads with Fast-AP (Fermentas) and radiolabeled with ^{32}Pγ-ATP using T4 PNK (NEB). Beads were washed another 4 times with Wash buffer supplemented with 4 M urea. Finally, samples were separated on a 4–12% gradient SDS-PAGE (Life Technologies) and transferred onto nitrocellulose membrane (GE Healthcare). RNA–protein complexes were visualized on film. Pieces of membrane between 125 and 225 kDa, corresponding to Ago2-bound RNAs up to 300 nucleotides, were excised and incubated in PK/urea buffer containing 4 mg of proteinase K (Roche). RNAs were extracted using TRIzol LS (Life technologies) as described earlier and precipitated with ethanol: isopropanol (1:1) and 1 μl of GlycoBlue (Ambion). cDNA libraries were prepared using the TruSeq small RNA sample kit (Illumina). cDNAs were amplified by 15 cycles of PCR and run on a TBE-urea polyacrylamide gel. Products ranging from 145 to 200 base pairs (corresponding to cDNA fragments between 20 and 75 base pairs without the adapters) were excised and recovered. The quality of the libraries was assessed with Agilent Technologies Bioanalyzer and concentrations were measured by qPCR using Kapa Library Quantification Kit (Kapabiosystems). cDNA libraries were sequenced by the

Downloaded from https://academic.oup.com/nar/article/45/7/4158/2726865 by BIU Montpellier user on 14 June 2022

MGX core facility (Montpellier GenomiX) on an Illumina HISeq2000 with 50 nucleotides run length.

Data analysis

Reads of low quality were discarded, adapter sequences were trimmed and sequences were sorted according to the specific barcodes used in each condition of IP using cutadapt software (https://cutadapt.readthedocs.org/en/stable/). Cleans reads were then mapped to HIV-1 NL4-3 sequence (GenBank ID: AF324493.2) or hg19 UCSC *H. sapiens* genome. In a first analysis, trimmed reads of at least 15 nucleotides length were mapped using Bowtie software (http://bowtie-bio.sourceforge.net/index.shtml with the following parameters: -a -n1 –best –strata). HITS-CLIP clusters were defined using Piranha software (39) with a 50 nucleotides bin, following a negative binomial distribution. Enrichment was determined by P-values < 0.05.

In a second analysis, we aim to rule out reads that could correspond to sncRNAs from viral origin present in the IP. For this, only reads to a range of 5 to 12 nucleotides without a perfect match to the 3′ adapter were considered. For subsequent analysis, we used a match of 7 nucleotides that give the best compromise for both adapters and long reads recognition. In order to find the best alignment parameters, long reads were aligned using Bowtie2 (http://bowtie-bio.sourceforge.net/bowtie2/) to the concatenation of the human and viral genome with variable combinations of seed substring (-L), tolerated mismatches per seed (-N) and interval between seed substring (-i). The best mapping statistics to the reference were obtained by using -L 3 -N 0 -i S,1,1.5, parameters tolerating mismatches that increased sensitivity but turned the alignment long to run. In order to exclude ambiguous reads, we aligned long reads to the human and viral genomes. Viral mappers not present in the human alignment were selected. Exclusively viral reads were mapped on each of HIV-transcripts using the -a option of Bowtie2. To identify HIV-1 clusters that are enriched in the IP, read coverage throughout the HIV genome was calculated, normalized by the number of hits and sequencing depth. For the calling of chimeras in HITS-CLIP data using hyb (40), HITS-CLIP reads were pre-processed selecting Flexbar preprocessing, trimming reads from 3′ end with a minimum read length of 17, then chimeras where called using hyb default parameters against a custom database of human and viral RNAs.

Dual Luciferase assay

HIV-1 clusters and controls as well as miR target sequences (Supplementary Tables S1 and S2) were inserted into PsiCHECK-2 vector (Promega) either by primer annealing or by PCR amplification. HEK293T and HeLa cells were transfected with PsiCHECK-2 constructs using FuGene 6 (Promega) and Lipofectamine LTX (Life Technologies), respectively. Seventy-two hours post-transfection, Renilla (RLuc) and Firefly (FLuc) luciferase activities were quantified using the Dual-Luciferase Reporter Assay System (Promega) on a BMG Labtech microplate reader. The mirVana miR92a inhibitor (ThermoFisher Scientific) or control were transfected in HEK293T cells using Lipofectamine RNAiMAX (Life Technologies) and 48 h later, cells were transfected with PsiCHECK-2 constructs. Relative Luciferase activity was assessed as described earlier.

HIV-1 RNA splicing and virus production

Dicer KO or Ago2 KO/ Ago1 KD cells were transfected with pNL4-3 plasmid using Lipofectamine LTX (Life Technologies), washed with 1X PBS 24 h later and cells and virus containing supernatants were collected 72 h after transfection. Level of CAp24 was quantified by ELISA in the cells extract and in the supernatant. Virus containing supernatants were used to infect HeLa TZM-bl indicator cells in serial dilutions. Twenty-four hours post-infection, whole cell lysates were assayed for induction of β-galactosidase expression using the Luciferase Assay System (Promega). Infectivity was expressed as Luciferase level normalized to the level of CAp24 quantified in the supernatant. Cell lysates were analyzed by immuno-blotting using anti-CAp24 (ARP366, National Institute for Biological Standards and Control (NIBSC)) and amounts of Gag products were quantified on a Fusion FX (Vilber Lourmat) apparatus. RNA was extracted from cells extracts using RNeasy Mini kit (QIAGEN), reverse transcribed and resulting cDNA was used to quantitate HIV mRNAs levels by real-time PCR using specific sets of primers for total RNA, unspliced, singly spliced and multiply spliced viral RNAs (Supplementary Table S3). For semi-quantitative PCR analysis, the same amount of total viral RNA was used for amplification with oligonucleotides primers specific for the 1.8-kb and 4-kb viral transcripts as described in (41). Amplification products were visualized on 1% agarose gels stained with Ethidium Bromide.

RESULTS

Ago2 binds to HIV-1 RNAs in infected cells

Several reports using RNA immunoprecipitation approaches recently showed that Ago2 interacts with HIV-1 RNAs in transfected cells (25,26,33). In order to further address the specificity of this interaction in infected cells, we used a CLIP assay that includes an *ex vivo* UV cross-linking step prior to cell lysis to capture RNA protein interactions in their native architecture and to minimize post-lysis re-association of miRNAs and mRNAs with Ago2 (42). CLIP of endogenous Ago2 was first performed from HIV-1 infected Jurkat T-lymphocyte cell line. RNAs bound to endogenous Ago2 were immunoprecipitated, purified and quantified by RT-qPCR. Similarly to what was previously observed in HEK293 cells (43), cellular IRF3 mRNA was co-immunoprecipitated with Ago2 in Jurkat cells (Figure 1). It was therefore used as a positive control of Ago2-IP. The US HIV-1 gRNA was efficiently co-immunoprecipitated with Ago2, at levels that were similar to IRF3 mRNA. On the contrary, the level of co-immunoprecipitated multiply spliced HIV-1 RNAs was more than 6-fold lower than the US HIV-1 gRNA (Figure 1), indicating that Ago2 preferentially binds to viral gRNA in HIV-1 infected Jurkat cells. A similar interaction was also observed in HEK293T and HeLa cells as well as in IP of Myc-tagged Ago2 and GFP-tagged Ago2 proteins (data not shown).

Downloaded from https://academic.oup.com/nar/article/45/7/4158/2726865 by BIU Montpellier user on 14 June 2022

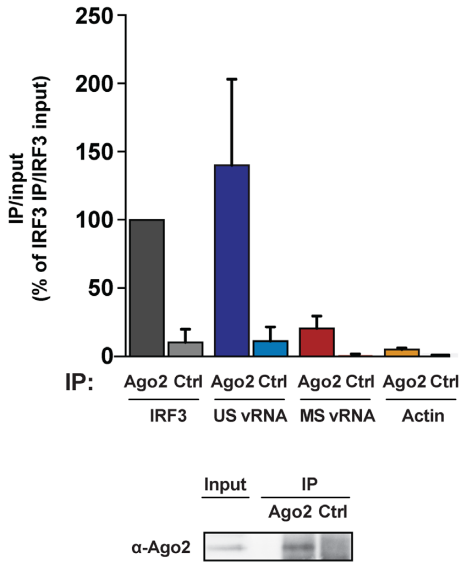


Figure 1. Ago 2 binds to HIV-1 RNAs in infected cells. Jurkat cells were infected with VSV-G-pseudotyped HIV NL4-3 at a multiplicity of infection (M.O.I.) of 1. Twenty-four hours later, cells were subjected to UV cross-linking and RNA–protein complexes were immunoprecipitated using an anti-Ago2 antibody or control IgGs. Immunoprecipitated (IPed) RNA was quantified by RTqPCR using primers specific for IRF3, unspliced (US) and multiply spliced (MS) HIV-1 RNAs, and Actin. IPed RNA values are presented as fraction of input RNA prior to immunoprecipitation (IP/input) and normalized to those of IRF3. Values are presented as means ± SD (n = 5). One-fifth of the sample was visualized by immunobloting using an anti-Ago2 antibody.

HITS-CLIP mapping of Ago2 binding regions on HIV-1 RNA

To precisely map the Ago2 binding regions on the HIV-1 RNA genome, we employed a high-resolution approach using high throughput sequencing of RNA isolated by CLIP. As high level of specificity during the IP is essential for HITS-CLIP, several antibodies against endogenous Ago2 and tagged versions of Ago2 protein were tested. Immunoprecipitation of the GFP-tagged Ago2 (GFP-Ago2) using an anti-GFP antibody and wash buffers supplemented with 4 M urea resulted in the most specific HIV RNA enrichment relative to control (data not shown). HITS-CLIP experiments were thus performed from GFP-Ago2 transfected 293T cells infected with VSVg pseudotyped HIV-1. Endogenous CAp24 staining and FACS analysis indicated that 75–90% of transfected cells were infected. Twenty-four hours after infection, cells were UV-irradiated at 254 nm to freeze RNA–proteins interactions as mentioned earlier. Whole cell lysates containing both cytoplasmic and nuclear fractions were digested by DNase treatment and 1/15th was kept for subsequent small library preparation (Input). The rest was subjected to partial RNAse I treatment and GFP immunoprecipitation was performed under highly stringent conditions. Immunopurified RNAs were radiolabeled, separated on SDS-PAGE and transferred to nitrocellulose membrane. Autoradiograms revealed the presence of RNA–protein complexes migrating from 125 kDa, the expected size of GFP-Ago2, to higher molecular weights corresponding to the size distribution of RNAs associated with GFP-Ago2 (Figure 2A). The levels of RNAs cross-linked to GFP-Ago2 were similar in presence or absence of infection but were highly enriched compared to the control GFP immunoprecipitation, confirming the specificity of our IP conditions. Ago2-RNA complexes migrating between 125 kDa and 225 kDa, corresponding to nucleic acids up to 300 nucleotides length, were extracted from the nitrocellulose membrane. Ago2 cross-linked RNAs were purified and reverse transcribed to generate small cDNA Illumina libraries. cDNA ranging from 20 to 75 base pairs were purified for subsequent deep sequencing. Libraries were also generated from GFP control samples. However, the levels of cDNA obtained from these samples were not sufficient for subsequent deep sequencing. High throughput sequencing was conducted on small RNA libraries generated from six independent Ago2-GFP HITS-CLIP experiments prepared from either uninfected or HIV-1 NL4-3 infected cells and their corresponding inputs. HITS-CLIP experiments yielded between 15 and 24 millions sequencing reads and inputs between 17 and 30 millions sequencing reads (Table 1).

Ago2 HITS-CLIP analysis

To assess the quality of our HITS-CLIP experiments, we first uploaded our sequencing reads to the CLIPZ software, specifically dedicated to HITS-CLIP data analysis (44). The number of distinct reads mapping to the human genome and the quality of the sequences were similar to other Ago2 HITS-CLIPs analyzed with the CLIPZ tool (data not shown). The alignment of reads in the input and in the HITS-CLIP experiments showed that whereas rRNAs, tRNAs and mRNAs were the predominant reads in the input (45%, 12% and 17%, respectively), a 2.5-fold enrichment of mRNAs, but not of snoRNAs, snRNAs, rRNAs or tRNAs, could be observed in the HITS-CLIP (Figure 2B). We did not observe any enrichment in miRNAs likely because our HITS-CLIP procedure favored long reads over short ones. We then sought to identify Ago2 binding sites on the viral gRNA. For this, HITS-CLIP data were analyzed in two different ways. First, trimmed reads longer than 15 nucleotides were aligned to the viral genome with a maximum of one mismatch allowed. Ago2 binding sequences were identified by overlapping reads and by identifying statistically significant peaks above background (cut-off of P-value < 0.05). The three HITS-CLIP experiments were highly reproducible and led to the identification of statistically significant clusters representing regions of HIV-1 RNA genome that were bound by Ago2 (Supplementary Figure S1). These sequences could either correspond to sncRNAs from viral origin that are loaded into Ago2 complexes or to Ago2 target sites on the viral genome. To identify Ago2 binding sites on the HIV-1 genome, we then refined our analysis: small trimmed reads of miRNA sizes (between 18 and 30 nt) were discarded and only long reads of 50 nucleotides were considered. Using a homemade pipeline based on Bowtie2, they were first aligned to the human and viral genome with parameters tolerating mismatches. In a second round, solely viral reads were mapped to the viral transcripts, with parameters tolerating mismatches. Searching for all possible alignments, we determined read coverage on HIV-1 genome normalized by the number of hits and se-

Downloaded from https://academic.oup.com/nar/article/45/7/4158/2726865 by BIU Montpellier user on 14 June 2022

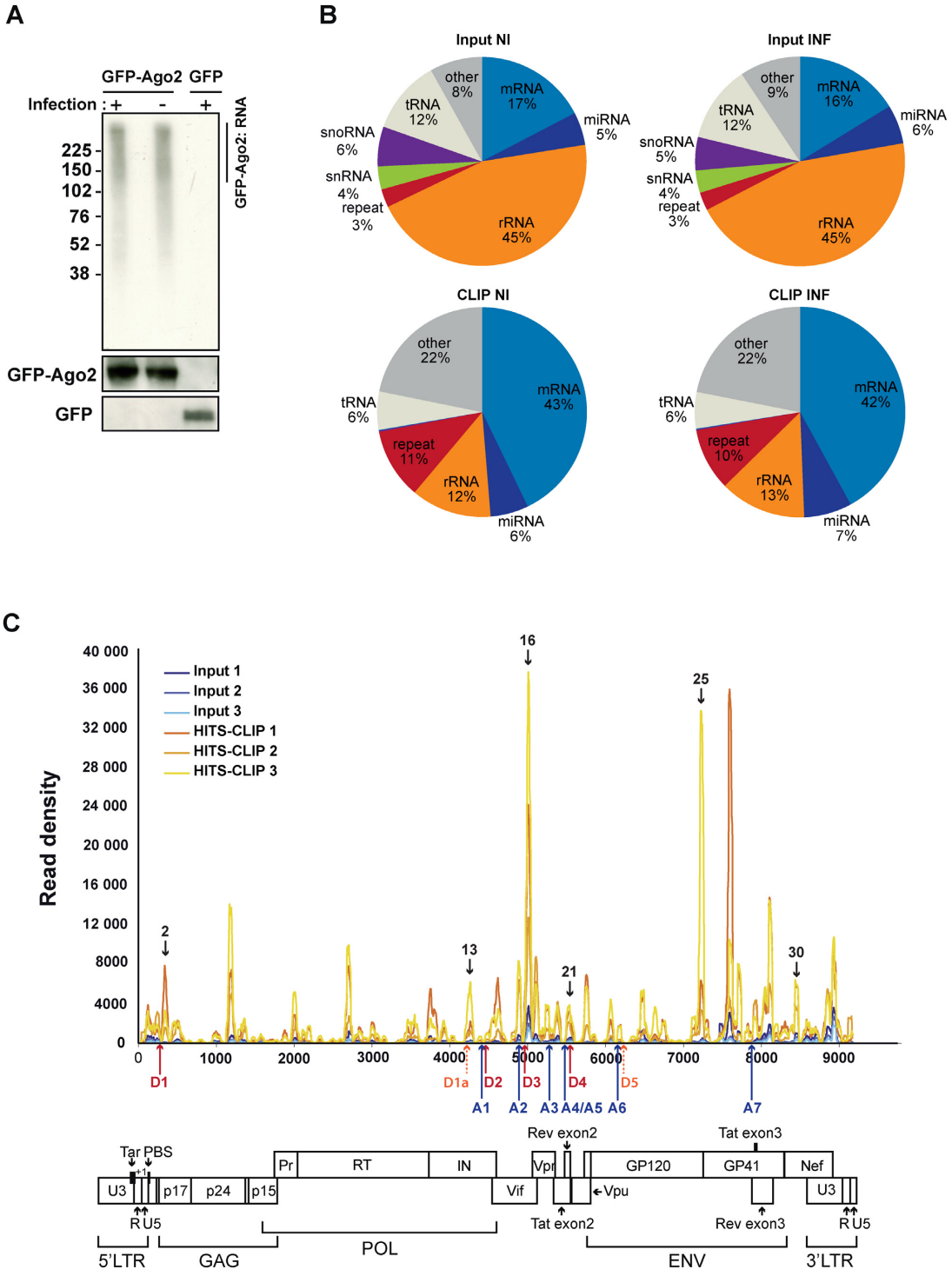


Figure 2. HITS-CLIP reveals HIV-1 regions bound by Ago2 in HIV-1 infected cells. (**A**) HEK293T cells were transfected with plasmid expressing either GFP-Ago2 or control GFP. Twenty-four hours later, they were infected with VSVg-pseudotyped HIV-1 NL4-3 at a M.O.I. of 1 or mock infected. Twenty-four hours later, cells were subjected to UV cross-linking and RNA–protein complexes were subjected to immunoprecipitation using an anti-GFP antibody. IPed RNA was radiolabeled with [γ-^{32}P]ATP and samples resolved on SDS-PAGE. Radiolabeled RNA was visualized by autoradiography. RNAs migrating at a higher molecular mass than the protein of interest (GFP-Ago2:RNA, between 125 and 225 kDa) were extracted from the membrane, reverse transcribed into cDNA and subjected to high throughput sequencing. (**B**) Reads obtained from non-infected (NI) and infected (INF) samples were uploaded to CLIPZ software. Reads that aligned to the human genome were sorted into categories: messenger RNA (mRNA), microRNA (miRNA), ribosomal RNA (rRNA), repeat, small non-coding RNA (snRNA), small nucleolar RNA (snoRNA), transfer RNA (tRNA) and other. Pie charts correspond to the distribution of the mean value of three biological replicates. (**C**) Reads obtained from infected samples were aligned to the HIV-1 NL4-3 sequence. Only reads $\geq$50 nucleotides length that aligned once without mismatch were considered for this analysis. Reads obtained from three independent HITS-CLIP experiments are presented in shades of orange and those obtained from the corresponding inputs in shades of blue. The map of the HIV-1 genome is presented below. Splice donor (D) and acceptor (A) sites are indicated. Peaks corresponding to clusters 2, 13, 16, 21, 25 and 30 are indicated by arrows.

Downloaded from https://academic.oup.com/nar/article/45/7/4158/2726865 by BIU Montpellier user on 14 June 2022

Table 1. Overview of Input and Ago2 HITS-CLIP libraries analyzed

	Raw reads[a]	Long reads[b] (>50 nt)	Mapped reads[c] (viral and human)	Human reads[d]	Viral reads[e]	Viral reads[f] (%)
Input NI-1	29 137 393	7 032 622	5 149 468	5 149 431	37	0.0007
Input NI-2	21 300 694	6 409 883	4 975 413	4 975 370	43	0.0009
Input NI-3	17 054 506	5 838 978	4 494 867	4 494 834	33	0.0007
Input INF-1	29 770 061	7 421 651	5 630 864	5 576 248	54 616	0.97
Input INF-2	20 803 549	5 475 336	4 158 674	4 131 255	27 419	0.66
Input INF-3	23 078 959	7 219 948	5 719 199	5 699 776	19 423	0.34
HITS-CLIP NI-1	15 914 798	3 234 726	932 011	931 378	633	0.07
HITS-CLIP NI-2	18 694 075	3 464 826	1 006 016	1 005 525	491	0.05
HITS-CLIP NI-3	24 112 728	7 043 654	3 289 780	3 289 516	264	0.01
HITS-CLIP INF-1	20 467 291	4 880 930	1 243 965	933 335	310 630	24.97
HITS-CLIP INF-2	20 288 674	5 267 660	2 217 001	2 041 903	175 098	7.90
HITS-CLIP INF-3	17 429 237	5 220 204	2 616 627	2 258 067	358 560	13.70

[a]Number of high quality reads obtained from the sequencing of each library.
[b]Number of reads longer than 50 nucleotides.
[c]Number of reads that aligned either to NL4-3 HIV-1 sequence (GenBank ID: AF324493.2) or to the hg19 UCSC *H. sapiens* genome.
[d]Number of reads that aligned exclusively to the human genome.
[e]Number of reads that aligned exclusively to NL4-3 HIV-1 sequence.
[f]Percentage of reads that aligned to NL4-3 HIV-1 sequence amongst the total number of reads assignable either to HIV-1 sequence or to human genome (Column c).

quencing depth. The numbers of reads obtained after each step of this analysis are summarized in Table 1. The few reads detected in the non-infected samples may be due to small contaminations during the HITS-CLIP procedure, library preparation or deep sequencing. Less than 1% of the total reads mapped to HIV-1 genome in the inputs, 99% being from cellular origin. After Ago2 IP, between 8 and 25% of the reads mapped to HIV-1 sequences indicating that, in our HITS-CLIP conditions, HIV-1 RNAs were enriched after Ago2 IP. All HIV-derived reads proved to be in the sense orientation in the input and in the HITS-CLIP.

The number of reads represented at each position (nucleotides) of the HIV-1 RNA genome (starting at the transcription start site) from the three HITS-CLIPs (in orange) and their corresponding input (in blue) were plotted (Figure 2C). As the R region is present at both ends of the viral genome, the reads could not therefore be assigned unambiguously to the 3′ or 5′ ends. They were arbitrarily assigned at the 3′ end of the viral genome. Several HIV-1 peaks were detectable in the input but whether they correspond to small RNA produced by the virus or degradation products was unclear. In Ago2 HITS-CLIP, we identified 40 discrete Ago2 binding sites along the viral genome with an accumulation of clusters at the central region and the 3′ end of the genome (Figure 2C). Both analyses of our HITS-CLIP data gave very similar results as shown by the comparison of their mean traces (Supplementary Figure S2). We focused our interest on 31 clusters of reads based on the reproducibility of the peaks in the three HITS-CLIP experiments and the enrichment of reads in the IP over the input (Supplementary Figure S3 and Supplementary Table S1).

Functional validation of specific Ago binding sites in the HIV-1 genome

To further characterize Ago binding to HIV-1 regions identified by HITS-CLIP, the HIV-1 regions corresponding to the 31 clusters were tested using a Luciferase reporter assay. The psiCHECK-2 vector is commonly used to test the effect of miRNA-mediated post-transcriptional regulation on target genes. Binding of Ago proteins to a predicted miRNA targeting sequence cloned in 3′UTR of the Renilla Luciferase (RLuc) gene generally induces translation inhibition of its transcript and repression of RLuc expression. The vector also encodes a Firefly Luciferase (FLuc) under an HSV-TK promoter that is used to normalize RLuc expression to the level of transfection for each construct. The 31 putative HIV-1 Ago2 binding sequences were thus cloned at the 3′ end of the RLuc indicator gene in the psiCHECK-2 reporter plasmid (Supplementary Table S1). In addition, perfect target sites of miR-10a, miR-92a and miR-21 as well as HIV regions not identified in our HITS-CLIP (Ctrl1, 2 and 3) were used as controls. PsiCHECK-2 indicator plasmids were transfected in HEK293T cells with the assumption that binding of Ago2 to viral RNA clusters identified in the HITS-CLIP experiments should lead to the downregulation of RLuc expression. Results for each construct are expressed as a percentage of RLuc to FLuc ratio as compared to empty psiCHECK-2 vector. We identified six HIV-1 Ago2 binding regions (clusters 2, 13, 16, 21, 25 and 30) that showed a robust downregulation of RLuc expression (from 36 to 92% decrease, Figure 3A). As positive controls, the insertion of complementary binding sequences for endogenous miR-10a and miR-92a lead to a strong inhibition of RLuc expression (64 to 86% decrease, respectively). The use of an anti-miR-92a inhibitor fully restored RLuc expression of the psiCHECK-2 miR-92a reporter plasmid, indicating that this specific downregulation depends on endogenous miR-92a-mediated loading of Ago-RISC. In sharp contrast, the miR-21 binding sequence did not repress RLuc expression, likely reflecting the low level of endogenous miR-21 expression in HEK293T cells (45). The other HIV cluster sequences tested showed either no significant changes of RLuc expression or a 2- to 3-fold increase compared to empty vector (data not shown), the latter possibly reflecting effects on RLuc transcripts expression or stability.

Downloaded from https://academic.oup.com/nar/article/45/7/4158/2726865 by BIU Montpellier user on 14 June 2022

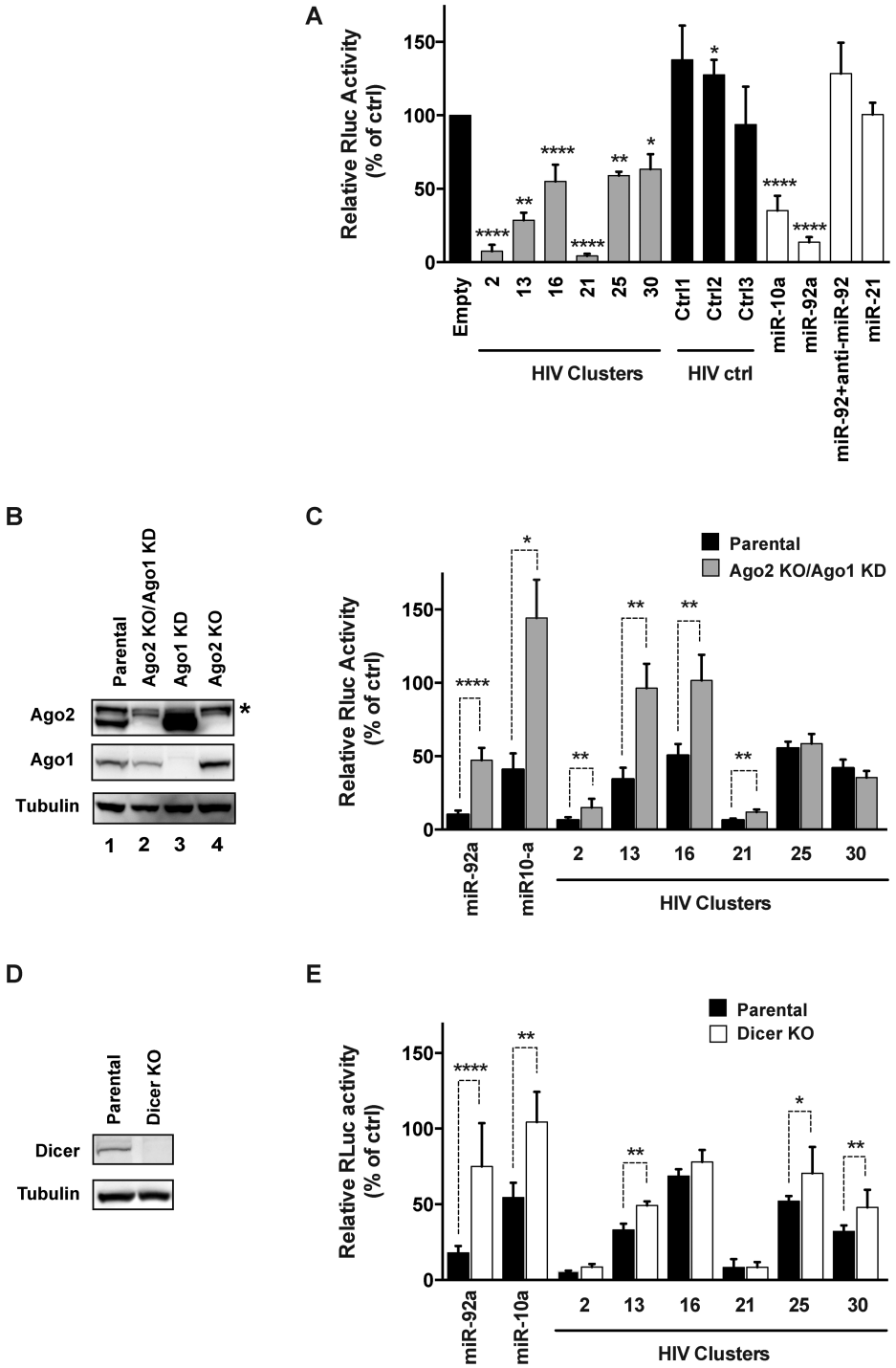


Figure 3. Functional validation of Ago2 binding regions of HIV-1. (**A**) HIV-1 clusters identified by HITS-CLIP experiments were inserted into psiCHECK-2 vector in 3′ of the RLuc indicator gene. Target sequences for cellular miR-10a, miR-92a and miR-21 were inserted as controls (in white) and HIV-1 sequences that were not identified as Ago2 targets by HITS-CLIP as negative controls (Ctrl1 to 3, in black). HEK293T cells were transfected with psiCHECK-2 constructs and luciferase activity was measured 72 h after transfection. RLuc activities were normalized to FLuc internal control and expressed as relative Rluc activity. Values are presented as percentage of the control psiCHECK-2 empty vector (Empty). Data are presented as mean of 3 to 9 replicates ±SD. HIV-1 clusters with Relative RLuc values that are significantly decreased as compared to the empty control are represented with grey bars. (**B**) Ago1 and Ago2 expression were monitored by immunoblotting using anti-Ago1 and anti-Ago2 antibodies. The star (*) indicates a non-specific band. (**C**) PsiCHECK-2 constructs containing HIV-1 or control sequences were transfected in parental (in black) or Ago2 knockout and Ago1 knockdown (Ago2 KO/Ago1 KD) (in grey) HeLa cells and RLuc/FLuc ratios were calculated as before (n = 3–8). *P*-values were calculated using a Student's *t*-test (****$P < 0.0001$, **$P < 0.01$ and *$P < 0.05$). (**D**) Dicer expression was monitored in parental and Dicer KO P4.2-HeLa cells by immunoblotting using an anti-Dicer antibody. (**E**) PsiCHECK-2 constructs containing HIV-1 sequences were transfected in parental (in black) or Dicer knockout (Dicer KO) (in white) P4.2-HeLa cells and RLuc/FLuc ratios were calculated as before (n = 3–7). *P*-values were calculated using a Student's *t*-test (****$P < 0.0001$, **$P < 0.01$ and *$P < 0.05$).

Downloaded from https://academic.oup.com/nar/article/45/7/4158/2726865 by BIU Montpellier user on 14 June 2022

In order to verify that downregulation of RLuc expression observed for clusters 2, 13, 16, 21, 25 and 30 was dependent on Ago proteins, the reporter assay was conducted in Ago downregulated cells. We first generated an Ago2 knockout (Ago2 KO) HeLa cell line using a CRISPR targeting exon 2 of the *Ago2* gene. Depletion of Ago2 expression was confirmed by immunoblot analysis (Figure 3B, lane 4 versus 1). Noticeably, Ago2 KO led to an increase in Ago1 protein levels as compared to control cells. Since Ago proteins have overlapping roles in cells, we also knocked-down the expression of Ago1 by using a specific shRNA. Transduction of HeLa cells with Ago1 shRNA efficiently silenced Ago1 protein expression (Figure 3B, lane 3). In parallel, an increase of Ago2 level was observed (Figure 3B, lane 3 versus 1). A similar compensation between Ago1 and Ago2 levels has been previously described (46). Transduction of Ago1 shRNA into Ago2 KO cells (Ago2 KO/ Ago1 KD), led to a decrease in Ago1 in absence of Ago2 expression (Figure 3B, lane 2 versus 1).

In these cells, we observed a derepression of RLuc expression from 3.5- to 4.6-fold for miR-10a and miR-92a, respectively (Figure 3C). Similarly, a 1.9- to 2.8-fold increase was observed for cluster 2, 13, 16 and 21, confirming a role of Ago proteins in the decrease of RLuc expression. In contrast, no effects for clusters 25 and 30 were observed (Figure 3C). Several HIV clusters that previously led to an upregulation of RLuc expression in control cells were also tested in Ago depleted cells. No effects were observed suggesting that the upregulation of RLuc expression in the psiCHECK-2 system was probably not depending on Ago proteins (data not shown).

Knocking down Ago expression could affect the expression of numerous cellular factors via the miRNA pathway and thus indirectly alter RLuc expression. One of the key functions of the Dicer endoribonuclease protein is to process pre-miRNA into mature mirRNA or dsRNA into siRNA. To investigate whether miRNA and siRNA are directly or indirectly involved in the repressive effects of clusters 2, 13, 16, 21, 25 and 30, we generated a *Dicer-null* HeLa-P4.2 cell line (HeLa cells expressing CD4+ and stably transfected with a LTR-β galactosidase reporter gene) using TALEN targeting the exon2 of *Dicer1* gene. Several Dicer-deficient cell clones were selected and we confirmed the loss of Dicer expression by immunoblot analysis (Figure 3D and data not shown). As expected, loss of Dicer resulted in derepression of RLuc expression from psiCHECK-2 vectors containing miR-92a and miR-10a target sites (1.9- to 4.8-fold, respectively) (Figure 3E). In sharp contrast, Dicer depletion had no impact on RLuc expression from clusters 2, 16 and 21. Whereas a limited derepression could be observed for clusters 13, 25 and 30, RLuc levels did not reach control levels (Figure 3E). These results indicate that cellular endogenous miRNAs processed by Dicer are either not or only partially required for RLuc downregulation mediated by HIV-1 clusters 2, 13, 16 and 21.

Altogether, these data indicate that the presence of cluster 2, 13, 16 and 21 in the 3′ UTR of RLuc can mediate the downregulation of the Luciferase expression through the presence of Ago proteins but largely independently of the miRNA pathway.

Ago2 is recruited to HIV-1 regions near functional splice donor sites

Strikingly, clusters 2, 13, 16 and 21 are in close proximity or overlap HIV-1 splicing donor sites D1, putative D1a, D3 and D4, respectively, whereas cluster 21 encompasses the A5 acceptor site (Figure 2C, Supplementary Figure S3 and Supplementary Table S1). To further investigate this observation, we cloned six HIV-1 acceptor and six donor splicing sites into psiCHECK-2 vector and tested their impact on RLuc expression (Supplementary Table S2). RLuc expression was specifically downregulated by the presence of splicing donor sites in its 3′UTR, in particular D1, putative D1a and D4 and to a lesser extent D3 and putative D5 but not D2. In sharp contrast, acceptor sites A2 to A7 showed either no effect or an increase in RLuc expression whereas acceptor site A1 displayed a modest reduction (Figure 4A).

Given the potential role of Ago proteins in regulating alternative splicing of cellular transcripts (13,15), we further assessed the effect of donor sites D1, D2, D3 and D4 when present in the context of the spliced junction sequences (Supplementary Table S2). Contrary to what we observed for the splicing donor sites alone, HIV-1 splice junction sequences inserted at the 3′ end of the RLuc gene had either no significant effect or stimulated RLuc expression (Figure 4B). We also re-analyzed our Ago2 HITS-CLIP data using 'hyb' bioinformatics pipeline that allows the mapping of chimeric RNAs in order to specifically detect clusters overlapping HIV-1 spliced junctions. HIV-1 reads containing unspliced junctions largely outnumbered reads corresponding to spliced transcripts (Table 2).

Mutations of the splicing donor sites of cluster 2, 13 and 16 were also tested in the RLuc reporter assay. Modification of the length of the inserted region induced a downregulation of RLuc activity as long as the donor site was present (Figure 4C, D, E, F and data not shown). A single mutation of the splice donor site (G/G to G/A), led to a complete derepression of the RLuc to FLuc ratio back to the control level. Similarly, the insertion of the sequence in an antisense orientation increased Rluc activity close to the empty control level indicating that the sequence rather than its secondary structure is important to mediate the repressive effect. Importantly, this repression is depending on the presence of a functional splice donor site. Furthermore, the downregulation of RLuc activity seems to correlate with the strength of the splice donor site as D1 and D4 are strong donor sites whereas D5 and D2 are relatively weak (2).

Repression of RLuc activity could be mediated through the recruitment of Ago proteins to the splice donor site in the luciferase 3′UTR and inhibition of translation as for the miRNA-dependent binding of Ago. Alternatively, introducing a splicing donor site in 3′UTR of RLuc could lead to an aberrant splice transcript using a downstream cryptic acceptor site, splicing out for instance the polyA tail. The HIV-1 5′ splice donor site could also suppress usage of the polyA signal site (47). Recruitment of the spliceosome without proper splicing could also lead to aberrant transcript and a subsequent degradation. To investigate further these possibilities, the level of RLuc and Fluc transcripts were measured for different constructs by RT-qPCR. Although a decrease in RLuc/FLuc ratio at the transcripts

Downloaded from https://academic.oup.com/nar/article/45/7/4158/2726865 by BIU Montpellier user on 14 June 2022

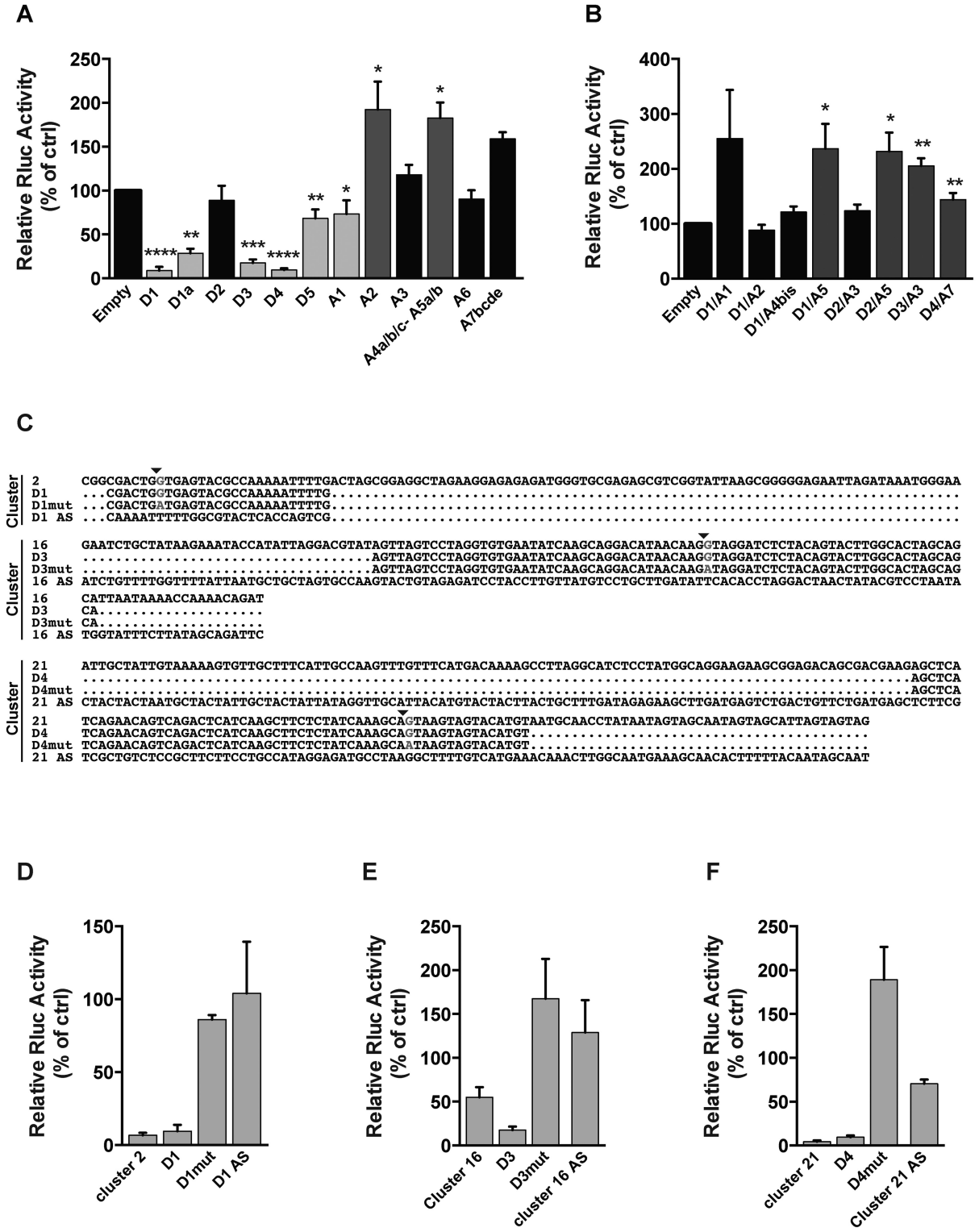


Figure 4. Ago2 binds to regions of HIV-1 near functional splice donor sites. (**A**) HIV-1 sequences encompassing either splice donor (D) or acceptor (A) sites (Supplementary Table S2) were cloned into psiCHECK-2 vector and relative RLuc/Fluc ratio was calculated as before. (**B**) HIV-1 sequences resulting from spliced junctions (Donor/Acceptor: D/A) were inserted into psiCHECK-2 and relative RLuc activity was measured as before. (**C**) HIV-1 clusters 2, 16 and 21 and truncated sequences encompassing the corresponding 5′ splice donor sites (SD), either wild-type (D), mutated on the SD site (Dmut) or in the antisense orientation (AS) were cloned into psiCHECK-2 vector. Splice donor sites are indicated by a black arrow. (**D, E** and **F**) PsiCHECK-2 constructs described in (C) were transfected in HEK293T cells and RLuc/Fluc ratio was calculated as before. Values are presented as percentage of the control psiCHECK-2 empty vector (Empty). Data are presented as mean of 3 to 9 replicates ± SD. *P*-values were calculated using a Student's *t*-test (****$P < 0.0001$, ***$P < 0.001$, **$P < 0.01$ and *$P < 0.05$).

Downloaded from https://academic.oup.com/nar/article/45/7/4158/2726865 by BIU Montpellier user on 14 June 2022

Table 2. Overview of the number of reads overlapping HIV-1 splice donor sites in Ago2 HITS-CLIP libraries

	Reads	NL4-3 Sequence
D1 unspliced	1271	**GGCGACTG GTGAGTACGCCAAAAAT**
D1/A1	50	**GGCGACTG** / GGACAGCAGAGATCCAGTTG
D1/A2	54	**GGCGACTG** / AATGTGCTATAAGAAATACCATA
D1/A3	9	**GGCGACTG** / AATTGGGTGTCGACATAGC
D1/A4c	2	**GGCGACTG** / TTTGTTTCATGACAAAAGCCTT
D1/A4a	8	**GGCGACTG** / CCTTAGGCATCTCCTATGGCAGG
D1/A4b	28	**GGCGACTG** / GCATCTCCTATGGCAGGATGG
D1/A5	146	**GGCGACTG** / GAAGAAGCGGAGACAGCG
D1/A5a	8	**GGCGACTG** / AAGCGGAGACAGCGACGAAGAGCT
D2 unspliced	1871	**TCTGGAAAG GTGAAGGGGCAGTA**
D2/A2	12	**TCTGGAAAG** / AATCTGCTATAAGAAATACCATAT
D2/A3	9	**TCTAGAAAG** / AATTGGGTGTCGACATAGCAGA
D2/A4a	2	**TCTGGAAAG** / CCTTAGGCATCTCCTATGGCAG
D2/A4b	3	**TCTGGAAAG**/GCATCTCCTATGGCATGAAGAAGCGGAG
D2/A5	24	**TCTGGAAAG** / GAAGAAGCGGAGACAGCGACGAA
D3 unspliced	72 938	**ATAACAAG GTAGGATCTCTACAGTACT**
D3/A3	1	**ATAACAAG** / AATTGGGTGTCGACATT
D3/A4b	1	**ATAACAAG** / GCATCTCCTATGGCAGGAAGAAGCG
D4 unspliced	2368	**TCAAAGCA GTAAGTAGTACATGTAA**
D4/A7	31	**TCAAAGCA** / ACCCACCTCCCAATCCCGAGG

Reads that encompass unspliced donor sites were aligned using Bowtie2 and reads that encompass spliced Donor sites were aligned using hyb as described in the Material and Methods section.

level could be seen for several splicing site containing constructs, we did not observed a correlation with the decreases in RLuc/Fluc protein activity ratio (Supplementary Figure S4A). Furthermore, no chimeric product between RLuc and Fluc transcripts could be amplified from cells transfected with the psiCHECK-2 plasmids containing clusters 2, 13, 16, 21 or the miR-92a binding sequence, suggesting that termination of RLuc and FLuc transcripts was not affected (Supplementary Figure S4B).

Taken together, our results show that HIV-1 Ago2 binding clusters that are located nearby HIV-1 splice donor sites present on the US HIV-1 RNA have the capacity to downregulate reporter gene expression through the presence of Ago proteins and in a miRNA independent manner.

Argonaute proteins participate to the regulation of HIV-1 multiply spliced RNA level

Given the close proximity of Ago binding clusters with HIV-1 splice donor sites and the suggested role of Ago proteins on alternative splicing of cellular transcripts, we sought to determine the effect of Ago proteins on multiply spliced HIV-1 transcript levels. Ago2 KO/Ago1 KD HeLa cells were first transfected with infectious HIV-1 plasmid pNL4-3 and 72 h post-transfection, total RNA was isolated from cells and reverse transcribed. Total viral RNA was quantified by quantitative PCR using primers specific for the U3-R region that is common to all HIV transcripts (Supplementary Table S3). The same amount of total viral RNA was used for each sample in subsequent analysis. Spliced viral mRNA species were first analyzed by semi-quantitative PCR and agarose gel analysis using primers detecting short multiply spliced 1.8-kb mRNAs and singly spliced 4-kb mRNAs (as described in (41)). A representative agarose gel of five independent experiments is shown in Figure 5A. Downregulation of Ago proteins resulted in an increase of MS 1.8-kb transcripts as compared to the control cells and a decrease in SS 4-kb mRNA. To assess the role of the miRNA pathway in viral pre-mRNA splicing regulation, the same experiment was performed in Dicer KO cells. Interestingly, SS 4-kb and MS 1.8-kb products were not substantially altered in absence of Dicer, suggesting that the effect of Ago proteins on HIV-1 process is independent on the miRNA pathway (Figure 5A).

We then analyzed viral mRNA by quantitative real-time PCR using sets of primers specific for US, SS and MS HIV-1 mRNAs. The level of each mRNA species was normalized to the level of total viral mRNA in each reaction. A primer set annealing immediately downstream of the major HIV-1 5′ SS (D1) was used to detect US Gag/Pol mRNA (Supplementary Table S3). Ago downregulation did not significantly affect the relative level of US viral mRNA (Figure 5B) or SS Env1/Vpu1 (D1∧A5) or Env/Vpu3 (D1∧A4a) mRNAs (Figure 5C). In contrast, when primers were used to detect MS mRNAs population that include splicing between D4 and A7, a 1.5-fold increase was observed in Ago2 KO/ Ago1 KD cells as compared to parental cells (Figure 5D). Furthermore, specific primer sets spanning different splice junctions were also used to detect Nef2 (D1∧A5/D4∧A7), Rev2 (D1∧A4a/D4∧A7) and Tat1 (D1∧A4/D4∧A7) (Supplementary Table S3) and again, downregulation of Ago proteins induced a significant 1.3- to 2-fold increase of these transcripts (Figure 5D). Importantly, Dicer KO did not significantly affect the level of US, SS or MS (Figure 5E, F and G, respectively) viral mRNAs, with the exception of Rev2 MS transcript downregulation, suggesting that the modulation of HIV MS transcripts relies on Ago proteins but is independent of the miRNA pathway.

Altogether, these data suggest that Ago proteins are involved in the processing of HIV-1 transcripts, by downregulating the levels of MS viral mRNAs in a Dicer independent manner.

Downloaded from https://academic.oup.com/nar/article/45/7/4158/2726865 by BIU Montpellier user on 14 June 2022

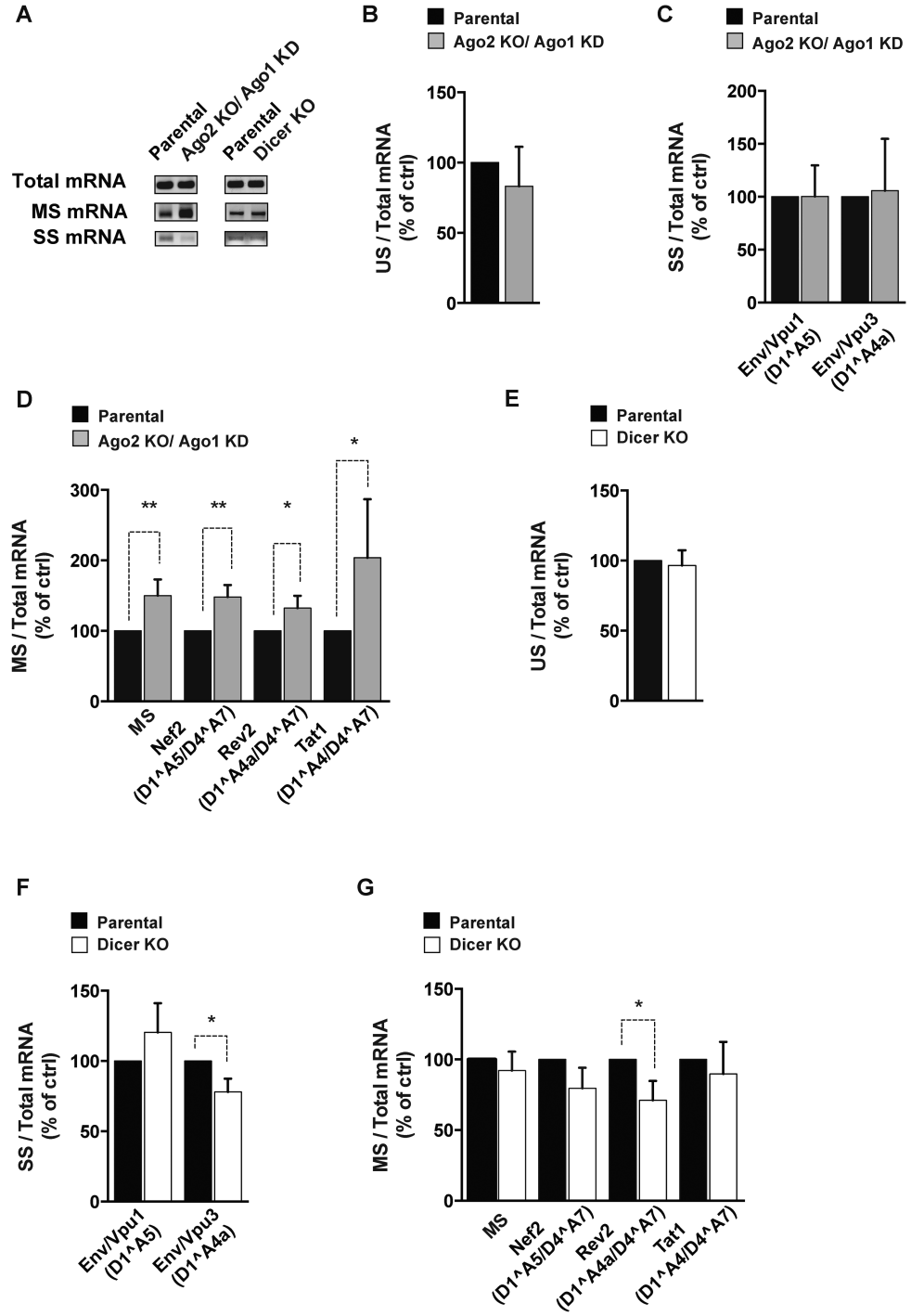


Figure 5. Knockdown of Ago1 in Ago2 knockout cells increases the level of multiply spliced HIV-1 transcripts independently on the miRNA pathway. (**A**) pNL4-3 provirus was transfected in Ago2 knockout and Ago1 knockdown (Ago2 KO/ Ago1 KD) HeLa cells and in Dicer knockout (Dicer KO) HeLa-P4.2 cells or their respective parental cells. Seventy-two hours later, RNA was extracted, reverse transcribed and total viral cDNA was quantified by qPCR using specific primers. Semi-quantitative PCR was performed on the same amount of total viral cDNA using primers specific for total, MS and SS HIV-1 mRNAs (see Supplementary Table S3 for primer sequences). Products of amplification were visualized on 1% agarose gel. A representative gel of five independent experiments is presented. (**B, C** and **D)** (US) (B), SS (C) or MS (D) mRNA isolated from Ago2 KO/ Ago1 KD cells were quantified by qPCR and their ratio to total viral RNA are indicated. Values are presented as percentage of the ratio in parental cells. Data are presented as mean of five replicates ± SD. (**E**) US, (**F**) SS or (**G**) MS mRNAs isolated from Dicer KO cells were quantified by qPCR and their ratio to total viral RNA are indicated. Values are presented as percentage of the ratio in parental cells. Data are presented as mean of four replicates ± SD. *P*-values were calculated using a Student's *t*-test (**$P < 0.01$ and *$P < 0.05$).

Downloaded from https://academic.oup.com/nar/article/45/7/4158/2726865 by BIU Montpellier user on 14 June 2022

Downregulation of Ago1 and Ago2 proteins impairs virus production

Since changes in the balanced splicing of HIV-1 mRNA can affect viral replication, we went on to determine the effect of Ago proteins, as well as of Dicer, on HIV-1 virion production. Ago2 KO/ Ago1 KD cells or Dicer KO cells were transfected with pNL4-3 proviral plasmid and HIV-1 production was assessed by ELISA quantification of the viral capsid (CAp24) protein in cells and in cell supernatants. Dicer KO did not drastically affect intracellular and extracellular CAp24 production, suggesting that the canonical miRNA pathway does not play a crucial role in HIV-1 RNA processing (Figure 6A and B). These results are in agreement with the study of Bogerd *et al*. (28). In contrast, intracellular Gag production was decreased by 40% in Ago downregulated cells (Figure 6C). In addition, Western blot quantification of Gag showed a reproducible 2-fold reduction in CAp24 to Pr55 and p41 to Pr55 ratios in Ago2 KO/ Ago1 KD cells as compared to control cells (Figure 6D). A similar Gag processing defect was previously reported in cells exhibiting excessive splicing (48,49). More importantly, extracellular Gag production was reduced by 10-fold in Ago2 KO/ Ago1 KD cell supernatants as compared to control cells (Figure 6E). Infectivity, defined as the level of infected cells to the level of CAp24 for each viral production, was only modestly affected with a 22% decrease as compared to control (Figure 6F). Altogether, these data indicate that Ago proteins positively regulate the production and release of viral particles, independently of the presence on the miRNA canonical pathway.

DISCUSSION

In this report, we used a CLIP and deep-sequencing approaches to identify Ago2 binding regions on HIV-1 RNAs. Our study revealed that in HIV-1 infected cells Ago2 interacts selectively with different regions on US viral RNA. Using a reporter assay, we found that Ago1 and Ago2 bind near HIV-1 splice donor sites in the context of the viral pre-mRNA. Furthermore, we showed that Ago proteins regulate the levels of multiply spliced viral transcripts. In addition, we showed that Ago1 and Ago2 expression are required for the production of viral particles. Importantly, these activities are independent on the miRNA processing RNAse Dicer.

We used the HITS-CLIP method to precisely map viral RNA regions targeted by Ago2 in HIV-1 infected HEK293T cells expressing GFP-Ago2 (Figure 2). Our study focused on HIV-1 RNA regions that correspond to Ago2 binding sites by only considering reads of 50 nucleotides length. We identified more than 40 reproducible binding sites distributed along the HIV-1 gRNA (Figure 2C). Remarkably, reads from viral origin represented <1% of the total reads in inputs, a result in agreement with other studies (22,30,32). In sharp contrast, between 8 to 25% of these long reads were from viral origin in our HITS-CLIP data, confirming that viral RNAs are preferentially enriched in Ago2 co-immunoprecipitation (Figure 1 and Table 1). Two recent reports have also explored the interaction between Ago proteins and HIV-1 RNAs

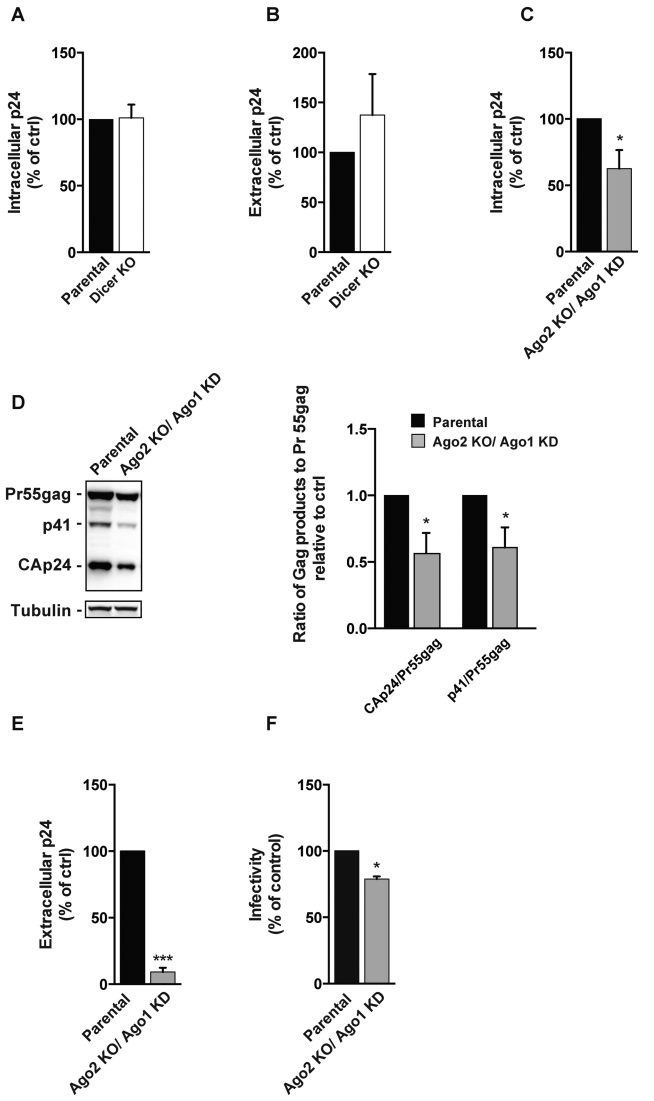


Figure 6. Knockdown of Ago1 in Ago2 knockout cells decreases the production of HIV-1 viral particles independently on the miRNA pathway. (**A**) Plasmid expressing wild-type HIV-1 NL4-3 virus was transfected in parental or in Dicer knockout (Dicer KO) HeLa-P4.2. Seventy-two hours later, intracellular CAp24 was quantified. Data are presented as mean of 3 replicates ± SD. (**B**) Production of virions was also quantified by measuring CAp24 in supernatants. Data are presented as mean of three replicates ± SD. (**C**) pNL4-3 provirus was transfected in parental or in Ago2 knockout and Ago1 knockdown HeLa cells (Ago2 KO/ Ago1 KD) HeLa cells. Seventy-two hours later, intracellular CAp24 was quantified. Values are presented as means ± SD (n = 3). (**D**) Western blot analysis of Gag products in Ago2 KO/Ago1 KD and parental HeLa cells and quantification of the precursor Pr55gag and p41 and CAp24 maturation products. CAp24 to Pr55gag ratio and of p41 to Pr55gag ratio are normalized to the ratio in parental cells. Data are presented as mean of five replicates ± SD. (**E**) Production of virions was quantified by measuring CAp24 in supernatants of parental or Ago2 KO/Ago1 KD HeLa cells transfected with plasmid expressing wild-type HIV NL4-3 virus. Values are presented as means ± SD (n = 3). (**F**) Infectivity of virions was measured by HeLa TZM-bl reporter assay and normalized to the quantity of CAp24 in the supernatants. Values are presented as means ± SD (n = 3). *P*-values were calculated using a Student's *t*-test (*$P < 0.05$).

Downloaded from https://academic.oup.com/nar/article/45/7/4158/2726865 by BIU Montpellier user on 14 June 2022

using similar photoactivable ribonucleoside-induced cross-linking and immunoprecipitation (PAR-CLIP) and HITS-CLIP approaches (22,32). Contrary to our study, Whisnant *et al*. detected very low levels of HIV-1 PAR-CLIP reads among the total of assignable reads (below 1%). This discrepancy could be due to differences in experimental conditions, as we used an overexpressed GFP-Ago2 together with stringent washing conditions in order to improve the efficiency and specificity of our immunoprecipitation conditions. Nevertheless, Whisnant *et al*. (22) identified a number of RISC clusters on HIV-1 RNA in infected TZM-bl HeLa and C8166 T cell lines. Importantly, our study identified 19 clusters that overlap with clusters identified in at least one of their two cell lines including cluster 2, 13, 16 and 21 (data not shown) indicating that these HIV-1 RNA regions are indeed conserved targets of endogenous Ago-RISC in different cell lines. In sharp contrast, viral RNAs were absent from Ago2-RISC in HIV-1 infected monocyte derived macrophages, suggesting that this interaction might be cell type specific (32).

To validate Ago HITS-CLIP targets, 31 of the HIV-1 clusters identified were tested in a 3′UTR reporter assay. In this assay, miRNA-mediated binding of Ago to the 3′UTR of the reporter gene induces downregulation of its expression. However, most of the clusters identified had either no effect or led to an upregulation of RLuc. Upregulation of transcripts expression through Ago binding to 3′UTR regions have been reported in some cases (50,51). However, when tested in Ago depleted cells, clusters leading to RLuc upregulation appeared to function independently of Ago proteins (data not shown). It is likely that the length of the inserted sequence, its secondary structure or the neighboring sequences introduced in 3′UTR of the Luciferase could stabilize the transcript or increase its translation as previously described (52). The fact that most of the Ago binding sites identified by HITS-CLIP had no effect in our reporter assay could be explained by the highly structured HIV-1 gRNA that was proposed to be refractory to the binding of miRNAs-Ago complexes (22,53,54). It is also possible that UV cross-linking procedure freeze interactions that are otherwise too labile to have an effect in the RLuc functional assay.

Nevertheless, we identified four HIV-1 clusters that were able to downregulated RLuc activity and we showed that these effects were dependent on both Ago1 and Ago2 proteins (Figure 3A and B). Interestingly, these four HIV-1 clusters are in close proximity or overlap HIV-1 splice donor sites (Figure 2C). An enrichment of Ago binding sites near splice junctions has already been reported on cellular transcripts (14–16,55). How Ago is recruited to these regions remains unclear. Our data indicate that to be functional, Ago binding sites have to be within the context of the US viral RNA sequence (Figure 4B, D, E and F). Moreover, we showed that endogenous Ago2 interacts preferentially with US viral RNA in HIV-1 infected CD4+T cells (Figure 1 and Table 2), a result that was also observed by others (33). In addition, our results using Dicer knockout cells indicate that Ago2 binding sites capable of downregulating RLuc expression, namely cluster 2, 13,16 and 21 function for the most part in a Dicer-independent manner, supporting the idea that miRNAs and short interfering RNAs are not, or only partially, required for Ago binding to these HIV-1 sequences (Figure 3C). A similar miRNA independent interaction between Ago2 and pre-mRNA transcripts was described for Ago2 in Drosophila (16). Interactions between Ago proteins and components of the splicing machinery and splicing regulatory factors have been described (15,43,56,57) and could be involved in recruiting Ago near HIV-1 splice donors. Alternatively, it is possible that Ago directly bind specific sequences or RNA secondary structures (16,58,59).

Several reports indicate that, by interacting with pre-mRNA transcripts, Ago proteins could regulate alternative splicing (14–16,55). We further explored their role in HIV-1 splicing and showed that knockdown of Ago1 in Ago2 knockout cells increased the level of multiply spliced viral RNAs by 1.3- to 2-folds (Figure 5D). Although these effects may appear limited, it has to be emphasized that downregulation of Ago1 was incomplete in Ago2 KO cells due to the mutually regulated expression of both Ago1 and Ago2 (Figure 3B and (46)). As Ago downregulation may impact numerous cellular factors via the miRNA pathway, including splicing factors, it could therefore indirectly affect HIV splicing. To address this issue, we followed the impact of Dicer KO on HIV-1 splicing. In agreement with what was shown in Drosophila, our data suggests that Ago proteins regulate HIV-1 MS RNA levels independently of the canonical miRNA pathway (16). Interestingly, Ago1 has been previously described to regulate cancer-related alternative splicing events independently of Dicer (13). On the contrary, using the CD44 gene as a model, Dicer was found to be involved in the regulation of alternative splicing, although evidences for a role of guide RNA are still missing (15). Thus, similarly to what was observed for cellular transcripts, our data support a model where Ago binding near splice donor sites on viral genomic RNA influences the fate of multiply spliced HIV-1 RNA transcripts. Further experiments will be required to define more precisely the mechanisms involved.

A role for Ago and miRNAs during HIV-1 replication is still debated as only mild effects were observed in Ago and Dicer depleted cells (27,33). Whisnant *et al*. identified several Ago binding sites on HIV-1 RNA by PAR-CLIP. However, only few of them could be assigned to cellular miRNAs suggesting that HIV-1 must be largely refractory to inhibition by the cellular miRNA pathway (22). On the other hand, our results clearly indicate that simultaneous downregulation of Ago1 and Ago2 diminished by 10-fold the release of CAp24 in the supernatant of transfected cells (Figure 6E). One hypothesis to explain this difference could be that we used cells depleted for both Ago1 and Ago2. Indeed, downregulation of Ago1 or Ago2 alone was not sufficient to achieve a robust effect on viral particle release (data not shown). Differences in experimental settings could also account for these discrepancies. Phalora *et al*. assessed the role of Ago proteins from virus entry to the production of new viral particles by infecting cells depleted for Ago expression (27). On the contrary, we limited our study to the late steps of viral production (after integration of the viral genome) by transfecting cells with a proviral expression plasmid, therefore bypassing potential effects of Ago depletion on early steps of HIV replication.

Downloaded from https://academic.oup.com/nar/article/45/7/4158/2726865 by BIU Montpellier user on 14 June 2022

In addition to a decrease in viral particles release, a concomitant 2-fold decrease in intracellular CAp24 and a reproducible defect in Gag processing were also noticed (Figure 6C and D). Although Ago2 binding to viral RNA may interfere with other steps of the virus replication that were not assessed in this study, these features are reminiscent of what was observed when excessive splicing of viral RNA was artificially induced (48,49). Again, although we cannot exclude that miRNAs matured through a Dicer independent pathway or other non-coding RNAs may be involved, our data suggest that miRNAs are also dispensable for the functionality of Ago proteins in viral particles production.

Thus, we propose that Ago1 and Ago2 bind to the viral gRNA nearby splice donor sites, in a miRNA independent manner and modulate the production of MS HIV-1 RNA, therefore regulating positively the production of viral particles.

SUPPLEMENTARY DATA

Supplementary Data are available at NAR Online.

ACKNOWLEDGEMENTS

The authors are grateful to Hugues Parinello (MGX Platform, IGF, Montpellier), Franck Letourneur (Genom'IC core facility, Institut Cochin, Paris), Marc Lavigne (Institut Pasteur, Paris), Gordon Langsley (Institut Cochin, Paris) and all members of the Berlioz and Emiliani lab for helpful discussions. The authors greatly acknowledge Karine Bailly, Emmanuelle Maillard and Muriel Andrieu at the Cytometry and Immunobiology core facility, Institut Cochin. The authors thank Lars Dölken (Julius-Maximilians-Universität Würzburg, Germany) for his valuable input and Adam Whisnant (Julius-Maximilians-Universität Würzburg, Germany) and Bryan Cullen (Duke University, Durham, NC, USA) for sharing their data. The following reagents were obtained through the NIH AIDS Reagent Program, Division of AIDS, NIAID, NIH: TZM-bl from Dr John C. Kappes, Dr Xiaoyun Wu and Tranzyme Inc., pNL4-3 from Dr Malcolm Martin. HeLa P4.2 cells were obtained from Dr Marc Alison. LentiCRISPR v2 was a gift from Feng Zhang (Addgene plasmid # 52961) and pT7-EGFP-C1-HsAgo2 and pT7-EGFP-C1 were a kind gift of Elisa Izaurralde.

FUNDING

Agence Nationale de Recherche sur le Sida et les Hépatites (ANRS) [to S.G.M. and S.E]; Agence Nationale de Recherche (ANR) Investissement d'Avenir [ANR-II-INSB-0014 to M.C. and J-P.C.]; Association Française contre les Myopathies (AFM) [n°18566 to M.C. and J-P.C.]; Action Thématique et Incitative sur Programme (ATIP) Grant from CNRS and Sanofi [to H.S.]; A.E. was a post-doctoral fellowship recipient from ANRS; N.P. was a post-doctoral fellowship recipient from La Ligue Nationale Contre le Cancer; D.U. was a recipient of an Engineer fellowship from Sidaction. Funding for open access charge: Institut National de la Santé et de la Recherche Médicale.
Conflict of interest statement. None declared.

REFERENCES

1. Ocwieja,K.E., Sherrill-Mix,S., Mukherjee,R., Custers-Allen,R., David,P., Brown,M., Wang,S., Link,D.R., Olson,J., Travers,K. *et al.* (2012) Dynamic regulation of HIV-1 mRNA populations analyzed by single-molecule enrichment and long-read sequencing. *Nucleic Acids Res.*, **40**, 10345–10355.
2. Stoltzfus,C.M. (2009) Chapter 1. Regulation of HIV-1 alternative RNA splicing and its role in virus replication. *Adv. Virus Res.*, **74**, 1–40.
3. Tazi,J., Bakkour,N., Marchand,V., Ayadi,L., Aboufirassi,A. and Branlant,C. (2010) Alternative splicing: regulation of HIV-1 multiplication as a target for therapeutic action. *FEBS J.*, **277**, 867–876.
4. Meister,G. (2013) Argonaute proteins: functional insights and emerging roles. *Nat. Rev. Genet.*, **14**, 447–459.
5. Benhamed,M., Herbig,U., Ye,T., Dejean,A. and Bischof,O. (2012) Senescence is an endogenous trigger for microRNA-directed transcriptional gene silencing in human cells. *Nat. Cell Biol.*, **14**, 266–275.
6. Kim,D.H., Villeneuve,L.M., Morris,K.V. and Rossi,J.J. (2006) Argonaute-1 directs siRNA-mediated transcriptional gene silencing in human cells. *Nat. Struct. Mol. Biol.*, **13**, 793–797.
7. Morris,K.V. (2006) Therapeutic potential of siRNA-mediated transcriptional gene silencing. *Biotechniques*, **Suppl**, 7–13.
8. Place,R.F., Li,L.C., Pookot,D., Noonan,E.J. and Dahiya,R. (2008) MicroRNA-373 induces expression of genes with complementary promoter sequences. *Proc. Natl. Acad. Sci. U.S.A.*, **105**, 1608–1613.
9. Chu,Y., Yue,X., Younger,S.T., Janowski,B.A. and Corey,D.R. (2010) Involvement of argonaute proteins in gene silencing and activation by RNAs complementary to a non-coding transcript at the progesterone receptor promoter. *Nucleic Acids Res.*, **38**, 7736–7748.
10. Huang,V., Zheng,J., Qi,Z., Wang,J., Place,R.F., Yu,J., Li,H. and Li,L.C. (2013) Ago1 Interacts with RNA polymerase II and binds to the promoters of actively transcribed genes in human cancer cells. *PLoS Genet.*, **9**, e1003821.
11. Gao,M., Wei,W., Li,M.M., Wu,Y.S., Ba,Z., Jin,K.X., Li,M.M., Liao,Y.Q., Adhikari,S., Chong,Z. *et al.* (2014) Ago2 facilitates Rad51 recruitment and DNA double-strand break repair by homologous recombination. *Cell Res.*, **24**, 532–541.
12. Wei,W., Ba,Z., Gao,M., Wu,Y., Ma,Y., Amiard,S., White,C.I., Rendtlew Danielsen,J.M., Yang,Y.G. and Qi,Y. (2012) A role for small RNAs in DNA double-strand break repair. *Cell*, **149**, 101–112.
13. Allo,M., Buggiano,V., Fededa,J.P., Petrillo,E., Schor,I., de la Mata,M., Agirre,E., Plass,M., Eyras,E., Elela,S.A. *et al.* (2009) Control of alternative splicing through siRNA-mediated transcriptional gene silencing. *Nat. Struct. Mol. Biol.*, **16**, 717–724.
14. Allo,M., Agirre,E., Bessonov,S., Bertucci,P., Gomez Acuna,L., Bellora,N., Singh,B., Petrillo,E., Blaustein,M. *et al.* (2014) Argonaute-1 binds transcriptional enhancers and controls constitutive and alternative splicing in human cells. *Proc. Natl. Acad. Sci. U.S.A.*, **111**, 15622–15629.
15. Ameyar-Zazoua,M., Rachez,C., Souidi,M., Robin,P., Fritsch,L., Young,R., Morozova,N., Fenouil,R., Descostes,N., Andrau,J.C. *et al.* (2012) Argonaute proteins couple chromatin silencing to alternative splicing. *Nat. Struct. Mol. Biol.*, **19**, 998–1004.
16. Taliaferro,J.M., Aspden,J.L., Bradley,T., Marwha,D., Blanchette,M. and Rio,D.C. (2013) Two new and distinct roles for Drosophila Argonaute-2 in the nucleus: alternative pre-mRNA splicing and transcriptional repression. *Genes Dev.*, **27**, 378–389.
17. Klase,Z., Houzet,L. and Jeang,K.T. (2012) MicroRNAs and HIV-1: complex interactions. *J. Biol. Chem.*, **287**, 40884–40890.
18. Houzet,L., Yeung,M.L., de Lame,V., Desai,D., Smith,S.M. and Jeang,K.T. (2008) MicroRNA profile changes in human immunodeficiency virus type 1 (HIV-1) seropositive individuals. *Retrovirology*, **5**, 118.
19. Triboulet,R., Mari,B., Lin,Y.L., Chable-Bessia,C., Bennasser,Y., Lebrigand,K., Cardinaud,B., Maurin,T., Barbry,P., Baillat,V. *et al.* (2007) Suppression of microRNA-silencing pathway by HIV-1 during virus replication. *Science*, **315**, 1579–1582.
20. Yeung,M.L., Bennasser,Y., Myers,T.G., Jiang,G., Benkirane,M. and Jeang,K.T. (2005) Changes in microRNA expression profiles in HIV-1-transfected human cells. *Retrovirology*, **2**, 81.

Downloaded from https://academic.oup.com/nar/article/45/7/4158/2726865 by BIU Montpellier user on 14 June 2022

21. Chang,S.T., Thomas,M.J., Sova,P., Green,R.R., Palermo,R.E. and Katze,M.G. (2013) Next-generation sequencing of small RNAs from HIV-infected cells identifies phased microrna expression patterns and candidate novel microRNAs differentially expressed upon infection. *MBio*, **4**, doi:10.1128/mBio.00549-12.
22. Whisnant,A.W., Bogerd,H.P., Flores,O., Ho,P., Powers,J.G., Sharova,N., Stevenson,M., Chen,C.H. and Cullen,B.R. (2013) In-depth analysis of the interaction of HIV-1 with cellular microRNA biogenesis and effector mechanisms. *MBio*, **4**, e000193.
23. Ahluwalia,J.K., Khan,S.Z., Soni,K., Rawat,P., Gupta,A., Hariharan,M., Scaria,V., Lalwani,M., Pillai,B., Mitra,D. *et al.* (2008) Human cellular microRNA hsa-miR-29a interferes with viral nef protein expression and HIV-1 replication. *Retrovirology*, **5**, 117.
24. Huang,J., Wang,F., Argyris,E., Chen,K., Liang,Z., Tian,H., Huang,W., Squires,K., Verlinghieri,G. and Zhang,H. (2007) Cellular microRNAs contribute to HIV-1 latency in resting primary CD4+ T lymphocytes. *Nat. Med.*, **13**, 1241–1247.
25. Nathans,R., Chu,C.Y., Serquina,A.K., Lu,C.C., Cao,H. and Rana,T.M. (2009) Cellular microRNA and P bodies modulate host-HIV-1 interactions. *Mol. Cell*, **34**, 696–709.
26. Chable-Bessia,C., Meziane,O., Latreille,D., Triboulet,R., Zamborlini,A., Wagschal,A., Jacquet,J.M., Reynes,J., Levy,Y., Saib,A. *et al.* (2009) Suppression of HIV-1 replication by microRNA effectors. *Retrovirology*, **6**, 26.
27. Phalora,P.K., Sherer,N.M., Wolinsky,S.M., Swanson,C.M. and Malim,M.H. (2012) HIV-1 replication and APOBEC3 antiviral activity are not regulated by P bodies. *J. Virol.*, **86**, 11712–11724.
28. Bogerd,H.P., Skalsky,R.L., Kennedy,E.M., Furuse,Y., Whisnant,A.W., Flores,O., Schultz,K.L., Putnam,N., Barrows,N.J., Sherry,B. *et al.* (2014) Replication of many human viruses is refractory to inhibition by endogenous cellular microRNAs. *J. Virol.*, **88**, 8065–8076.
29. Althaus,C.F., Vongrad,V., Niederost,B., Joos,B., Di Giallonardo,F., Rieder,P., Pavlovic,J., Trkola,A., Gunthard,H.F., Metzner,K.J. *et al.* (2012) Tailored enrichment strategy detects low abundant small noncoding RNAs in HIV-1 infected cells. *Retrovirology*, **9**, 27.
30. Schopman,N.C., Willemsen,M., Liu,Y.P., Bradley,T., van Kampen,A., Baas,F., Berkhout,B. and Haasnoot,J. (2012) Deep sequencing of virus-infected cells reveals HIV-encoded small RNAs. *Nucleic Acids Res.*, **40**, 414–427.
31. Yeung,M.L., Houzet,L., Yedavalli,V.S. and Jeang,K.T. (2009) A genome-wide short hairpin RNA screening of jurkat T-cells for human proteins contributing to productive HIV-1 replication. *J. Biol. Chem.*, **284**, 19463–19473.
32. Vongrad,V., Imig,J., Mohammadi,P., Kishore,S., Jaskiewicz,L., Hall,J., Gunthard,H.F., Beerenwinkel,N. and Metzner,K.J. (2015) HIV-1 RNAs are not part of the Argonaute 2 associated RNA interference pathway in macrophages. *PLoS One*, **10**, e0132127.
33. Bouttier,M., Saumet,A., Peter,M., Courgnaud,V., Schmidt,U., Cazevieille,C., Bertrand,E. and Lecellier,C.H. (2012) Retroviral GAG proteins recruit AGO2 on viral RNAs without affecting RNA accumulation and translation. *Nucleic Acids Res.*, **40**, 775–786.
34. Reed,J.C., Molter,B., Geary,C.D., McNevin,J., McElrath,J., Giri,S., Klein,K.C. and Lingappa,J.R. (2012) HIV-1 Gag co-opts a cellular complex containing DDX6, a helicase that facilitates capsid assembly. *J. Cell Biol.*, **198**, 439–456.
35. Huang,P., Xiao,A., Zhou,M., Zhu,Z., Lin,S. and Zhang,B. (2011) Heritable gene targeting in zebrafish using customized TALENs. *Nat. Biotechnol.*, **29**, 699–700.
36. Sanjana,N.E., Shalem,O. and Zhang,F. (2014) Improved vectors and genome-wide libraries for CRISPR screening. *Nat. Methods*, **11**, 783–784.
37. Jablonski,J.A. and Caputi,M. (2009) Role of cellular RNA processing factors in human immunodeficiency virus type 1 mRNA metabolism, replication, and infectivity. *J. Virol.*, **83**, 981–992.
38. Ule,J., Jensen,K., Mele,A. and Darnell,R.B. (2005) CLIP: a method for identifying protein-RNA interaction sites in living cells. *Methods*, **37**, 376–386.
39. Uren,P.J., Bahrami-Samani,E., Burns,S.C., Qiao,M., Karginov,F.V., Hodges,E., Hannon,G.J., Sanford,J.R., Penalva,L.O. and Smith,A.D. (2012) Site identification in high-throughput RNA-protein interaction data. *Bioinformatics*, **28**, 3013–3020.
40. Travis,A.J., Moody,J., Helwak,A., Tollervey,D. and Kudla,G. (2014) Hyb: a bioinformatics pipeline for the analysis of CLASH (crosslinking, ligation and sequencing of hybrids) data. *Methods*, **65**, 263–273.
41. Purcell,D.F. and Martin,M.A. (1993) Alternative splicing of human immunodeficiency virus type 1 mRNA modulates viral protein expression, replication, and infectivity. *J. Virol.*, **67**, 6365–6378.
42. Riley,K.J., Yario,T.A. and Steitz,J.A. (2012) Association of Argonaute proteins and microRNAs can occur after cell lysis. *RNA*, **18**, 1581–1585.
43. Landthaler,M., Gaidatzis,D., Rothballer,A., Chen,P.Y., Soll,S.J., Dinic,L., Ojo,T., Hafner,M., Zavolan,M. and Tuschl,T. (2008) Molecular characterization of human Argonaute-containing ribonucleoprotein complexes and their bound target mRNAs. *RNA*, **14**, 2580–2596.
44. Khorshid,M., Rodak,C. and Zavolan,M. (2011) CLIPZ: a database and analysis environment for experimentally determined binding sites of RNA-binding proteins. *Nucleic Acids Res.*, **39**, D245–252.
45. Tian,W., Dong,X., Liu,X., Wang,G., Dong,Z., Shen,W., Zheng,G., Lu,J., Chen,J., Wang,Y. *et al.* (2012) High-throughput functional microRNAs profiling by recombinant AAV-based microRNA sensor arrays. *PLoS One*, **7**, e29551.
46. Matsui,M., Li,L., Janowski,B.A. and Corey,D.R. (2015) Reduced expression of Argonaute 1, Argonaute 2 and TRBP changes levels and intracellular distribution of RNAi factors. *Sci. Rep.*, **5**, 12855.
47. Ashe,M.P., Griffin,P., James,W. and Proudfoot,N.J. (1995) Poly(A) site selection in the HIV-1 provirus: inhibition of promoter-proximal polyadenylation by the downstream major splice donor site. *Genes Dev.*, **9**, 3008–3025.
48. Mandal,D., Feng,Z. and Stoltzfus,C.M. (2008) Gag-processing defect of human immunodeficiency virus type 1 integrase E246 and G247 mutants is caused by activation of an overlapping 5′ splice site. *J. Virol.*, **82**, 1600–1604.
49. Mandal,D., Feng,Z. and Stoltzfus,C.M. (2010) Excessive RNA splicing and inhibition of HIV-1 replication induced by modified U1 small nuclear RNAs. *J. Virol.*, **84**, 12790–12800.
50. Mortensen,R.D., Serra,M., Steitz,J.A. and Vasudevan,S. (2011) Posttranscriptional activation of gene expression in Xenopus laevis oocytes by microRNA-protein complexes (microRNPs). *Proc. Natl. Acad. Sci. U.S.A.*, **108**, 8281–8286.
51. Vasudevan,S., Tong,Y. and Steitz,J.A. (2007) Switching from repression to activation: microRNAs can up-regulate translation. *Science*, **318**, 1931–1934.
52. Sun,G. and Rossi,J.J. (2009) Problems associated with reporter assays in RNAi studies. *RNA Biol.*, **6**, 406–411.
53. Tan,X., Lu,Z.J., Gao,G., Xu,Q., Hu,L., Fellmann,C., Li,M.Z., Qu,H., Lowe,S.W., Hannon,G.J. *et al.* (2012) Tiling genomes of pathogenic viruses identifies potent antiviral shRNAs and reveals a role for secondary structure in shRNA efficacy. *Proc. Natl. Acad. Sci. U.S.A.*, **109**, 869–874.
54. Watts,J.M., Dang,K.K., Gorelick,R.J., Leonard,C.W., Bess,J.W. Jr., Swanstrom,R., Burch,C.L. and Weeks,K.M. (2009) Architecture and secondary structure of an entire HIV-1 RNA genome. *Nature*, **460**, 711–716.
55. Chu,Y., Wang,T., Dodd,D., Xie,Y., Janowski,B.A. and Corey,D.R. (2015) Intramolecular circularization increases efficiency of RNA sequencing and enables CLIP-Seq of nuclear RNA from human cells. *Nucleic Acids Res.*, **43**, e75.
56. Hock,J., Weinmann,L., Ender,C., Rudel,S., Kremmer,E., Raabe,M., Urlaub,H. and Meister,G. (2007) Proteomic and functional analysis of Argonaute-containing mRNA-protein complexes in human cells. *EMBO Rep.*, **8**, 1052–1060.
57. Meister,G., Landthaler,M., Peters,L., Chen,P.Y., Urlaub,H., Luhrmann,R. and Tuschl,T. (2005) Identification of novel argonaute-associated proteins. *Curr. Biol.*, **15**, 2149–2155.
58. Leung,A.K., Young,A.G., Bhutkar,A., Zheng,G.X., Bosson,A.D., Nielsen,C.B. and Sharp,P.A. (2011) Genome-wide identification of Ago2 binding sites from mouse embryonic stem cells with and without mature microRNAs. *Nat. Struct. Mol. Biol.*, **18**, 237–244.
59. Frohn,A., Eberl,H.C., Stohr,J., Glasmacher,E., Rudel,S., Heissmeyer,V., Mann,M. and Meister,G. (2012) Dicer-dependent and -independent Argonaute2 protein interaction networks in mammalian cells. *Mol. Cell. Proteomics*, **11**, 1442–1456.

Downloaded from https://academic.oup.com/nar/article/45/7/4158/2726865 by BIU Montpellier user on 14 June 2022